



Providing Choice & Value
Generic CT and MRI Contrast Agents

**FRESENIUS
KABI**

CONTACT REP

AJNR

**Giant cholesterol cysts of the petrous apex:
radiologic features.**

J T Latack, M D Graham, J L Kemink and J E Knake

AJNR Am J Neuroradiol 1985, 6 (3) 409-413

<http://www.ajnr.org/content/6/3/409>

This information is current as
of July 24, 2025.

Giant Cholesterol Cysts of the Petrous Apex: Radiologic Features

Joseph T. Latack¹
 Malcolm D. Graham²
 John L. Kemink²
 James E. Knake¹

Four cysts are described that expanded and destroyed the bone of the petrous apex. All patients with these cysts had a sensorineural hearing loss. Mild symptoms referable to cranial nerves VI, VII, IX, X, XI, and XII were seen also. The cysts range in size from 1.5 × 1.5 × 3 cm to 5 × 5 × 6 cm. Grossly and histologically, they were distinct from any lesions seen previously. The lesions were large and contained glistening brown, watery fluid filled with cholesterol crystals. The cyst wall was predominantly fibrous tissue without an epithelium. Minimal chronic inflammatory change and granuloma formation were present within and just outside the cyst wall. These cysts have been described as mastoid cysts, epidermoids, mucocoeles, and cholesterol granulomas; until now, they have not been recognized as a single distinct entity. A name emphasizing the pathologic characteristic of the lesion, *giant cholesterol cyst*, has been suggested. Distinguishing them from other petrous apex lesions preoperatively is difficult, but if the cystic nature of the lesion can be recognized or at least anticipated, more conservative surgery, such as simple drainage versus a more radical procedure, may be possible.

During a 4 year period, the most common primary lesion of the petrous apex seen at the University of Michigan Medical Center was a large cyst filled with cholesterol-rich fluid and lined by a fibrous capsule. These cysts have been described previously as variants of other lesions but not recognized as a single distinct entity. Our report discusses the clinical, pathologic, and radiographic findings of these cysts, emphasizing the distinctive features that necessitate their classification as a new clinical entity.

Materials and Methods

Four adult patients with cystic lesions of the petrous apex were evaluated with complex-motion tomography, angiography, and computed tomography (CT) before and after intravenous administration of contrast material. Thin-section high-resolution CT of the temporal bone was performed in three of the patients with a GE 8800 scanner [1]. Magnetic resonance (MR) imaging was performed in one patient using a Diconics unit with a 0.5 T superconductive magnet operating at 0.35 T. Images were obtained with a repetition time (TR) of 1.0 and 2.0 sec in the axial plane, 1.0 sec in the coronal plane, and 0.5 sec in the sagittal plane. The times to echo (TEs) for all images were 28 and 56 msec. Pathologic specimens and clinical records were reviewed.

Results

High-resolution CT and/or complex-motion tomography demonstrated spherical, lytic lesions centered in the petrous apex and ranging in size from 1.5 × 1.5 × 3 cm to 5 × 5 × 6 cm (figs. 1–4). None of the abnormalities was confined to the petrous apex, the smallest enlarging laterally along the posterior surface of the petrous bone to the internal auditory canal (fig. 1). The other lesions extended

Received July 18, 1984; accepted after revision October 16, 1984.

Presented in part at the annual meeting of the American Society of Neuroradiology, Boston, June 1984.

¹ Department of Radiology, Division of Neuroradiology, University of Michigan Hospitals, Ann Arbor, MI 48109. Address reprint requests to J. T. Latack.

² Department of Otolaryngology–Head and Neck Surgery, University of Michigan Hospitals, Ann Arbor, MI 48109.

AJNR 6:409–413, May/June 1985

0195–6108/85/0603–0409

© American Roentgen Ray Society

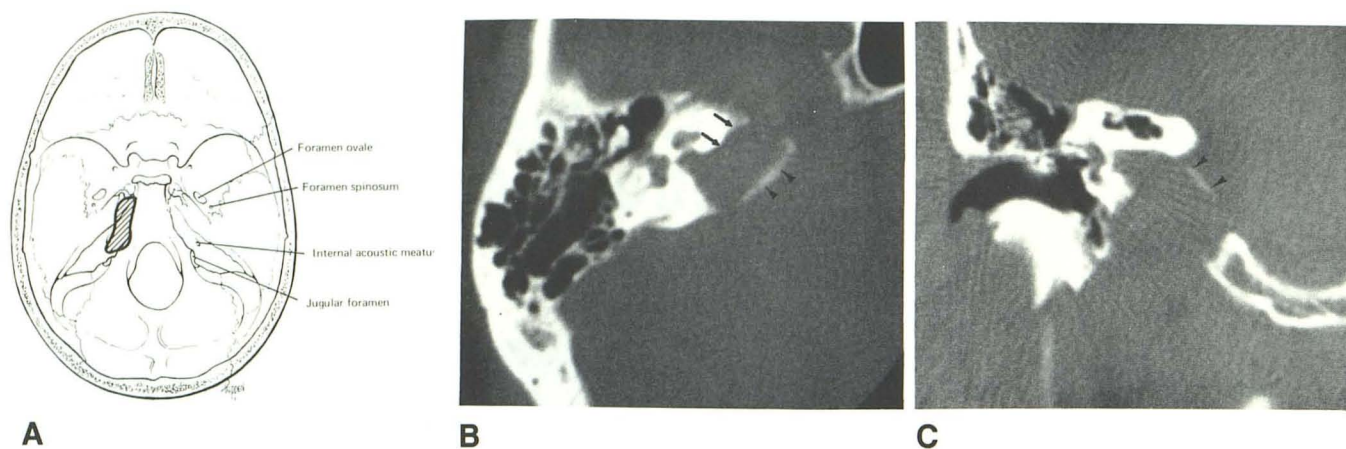


Fig. 1.—Smallest giant cholesterol cyst. **A**, Skull base viewed from above. Shaded area represents involvement of petrous apex and posterior surface of petrous bone to region of internal auditory canal. **B**, Axial high-resolution CT scan. Lytic lesion of petrous apex extending to internal auditory canal with

incomplete rim of thinned, elevated bone (arrowheads). Adjacent to otic capsule, bone is scalloped and sclerotic (arrows). **C**, Coronal scan. Destruction of bone below internal auditory canal. Incomplete bony rim around cyst medially (arrowheads).

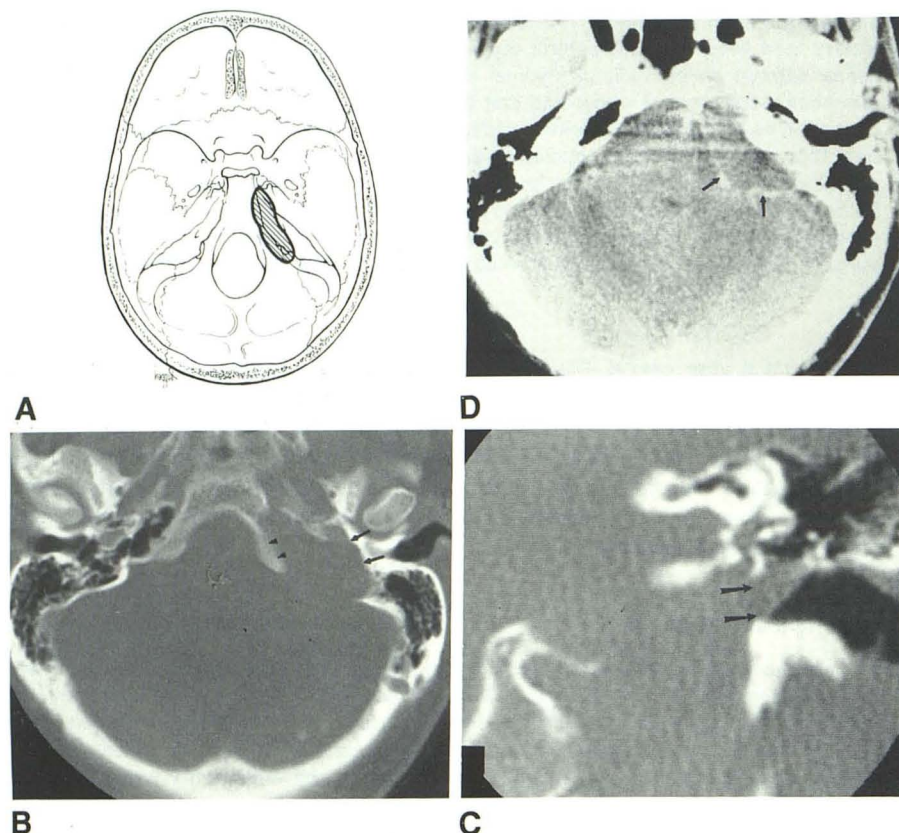


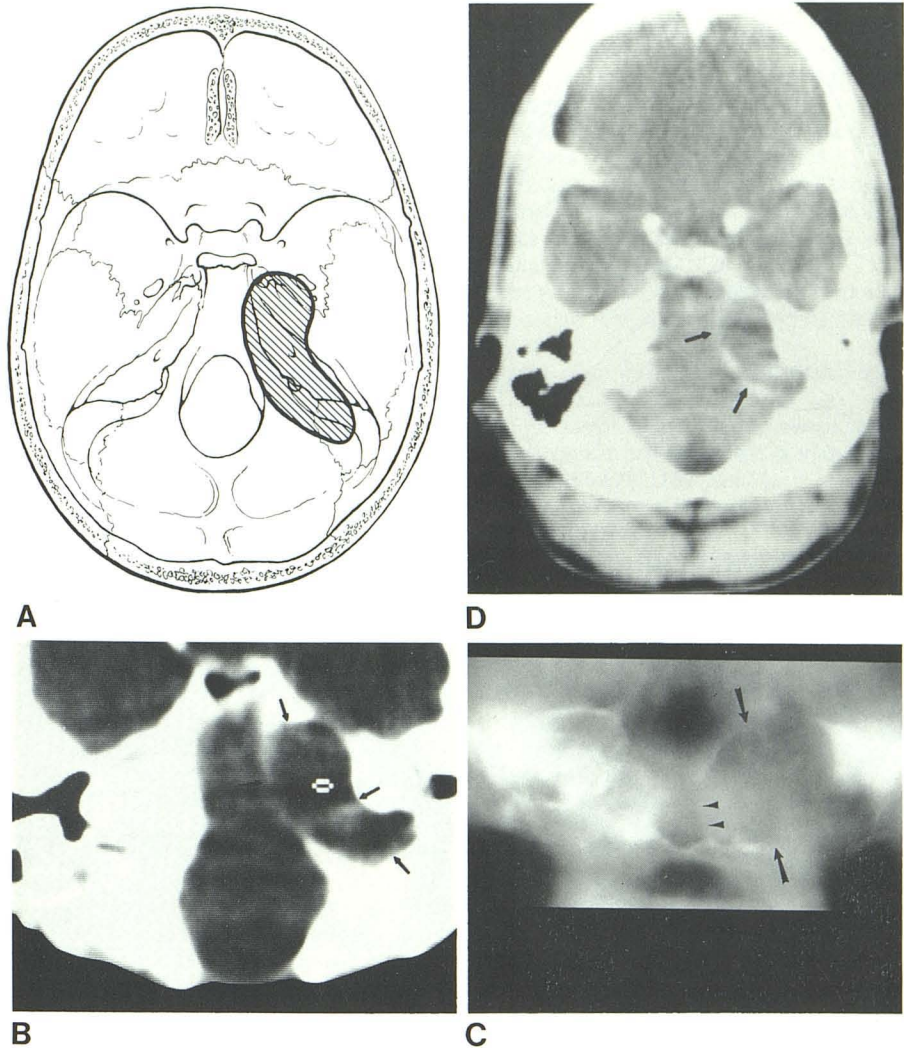
Fig. 2.—**A**, Shaded area represents giant cholesterol cyst of left petrous bone extending to region of jugular foramen. Occipital bone also involved. **B**, Axial high-resolution CT scan. Destruction of petrous apex and posterior surface of petrous bone with sclerotic, scalloped border laterally (arrows). Involvement of adjacent occipital bone (arrowheads). **C**, Coronal high-resolution CT scan. Destruction most marked again along inferior surface of petrous bone. Cyst breaks through posterior hypotympanum into middle ear cavity (arrows). **D**, Axial CT scan. Central part of cyst is of brain attenuation. Cyst wall enhances (arrows).

variable distances medially beyond the petrous bone, eroding parts of the occipital and/or sphenoid bone (figs. 2–4), and laterally beyond the internal auditory canal, destroying the bone of the cochlear aqueduct, jugular foramen, ascending part of the carotid canal (figs. 2–4), and the hypotympanum via the jugular canal (fig. 2C). The bone at the periphery of the lesion was sclerotic and scalloped laterally, adjacent to

the otic capsule (figs. 1B, 2B, 3C, and 4B), and elevated, expanded, and thinned into an incomplete bony rim elsewhere (figs. 1B, 3C, and 4C).

On CT with and without intravenous administration of contrast material, the central part of the lesion had an attenuation similar to that of brain (figs. 2D and 3D). After intravenous contrast material, rimlike enhancement of the periphery was

Fig. 3.—**A**, Largest giant cholesterol cyst (shaded area). Left petrous, sphenoid, and occipital bone involvement. **B**, Axial CT scan at bone windows. Destruction of petrous apex, posterior surface of petrous bone, and occipital bone (arrows). **C**, Coronal tomogram anterior to bony labyrinth. Lytic lesion with elevated, expanded, incomplete bony rim (arrows). Extension to sphenoid sinus (arrowheads). **D**, Axial CT scan. Interior of cyst of brain attenuation. Cyst wall enhances (arrows).



seen, projecting primarily into the posterior cranial fossa in all four patients (figs. 2D and 3D) and also into the middle cranial fossa in two patients.

In one patient, MR demonstrated a multilocular high-signal abnormality (fig. 4D). A smaller, similar lesion in the opposite petrous bone, detected initially by MR, but also present on CT, was not biopsied but was believed to represent the same entity.

Carotid and vertebral angiography in these patients revealed displacement of small arteries and veins adjacent to the petrous bone, but no displacement of the carotid artery or jugular vein. Vessel encasement and abnormal vascularity were not seen.

Clinically, all patients presented with a sensorineural hearing loss. Mild symptoms referable to cranial nerves VI, VII, IX, X, XI, and XII were also seen.

Pathologically, the lesions were large cysts, containing glistening brown, watery fluid filled with cholesterol crystals. The cyst wall was predominantly fibrous tissue without an epithelium. Minimal chronic inflammatory change and granu-

loma formation within and just outside the cyst wall were present.

Discussion

Review of the literature revealed that similar cysts of the temporal bone lined with fibrous tissue and containing cholesterol-rich fluid have been described in multiple reports as mastoid cysts [2, 3], epidermoids [4, 5], mucocoeles [6], and cholesterol granuloma [7, 8]. The cysts we are describing, as well as those in the above reports, did not contain squamous epithelium or debris as seen in congenital epidermoids, lacked the respiratory epithelium and mucus of a mucocoele, and were not solid lesions of the middle ear with numerous inflammatory cells and granulomas typical of the cholesterol granuloma [9–12]. Mastoid cyst is too anatomically limiting a name because our patients had petrous bone involvement with sparing of the mastoid. The gross and histologic characteristics of these cysts necessitate considering them a distinct new pathologic entity. A name emphasizing these

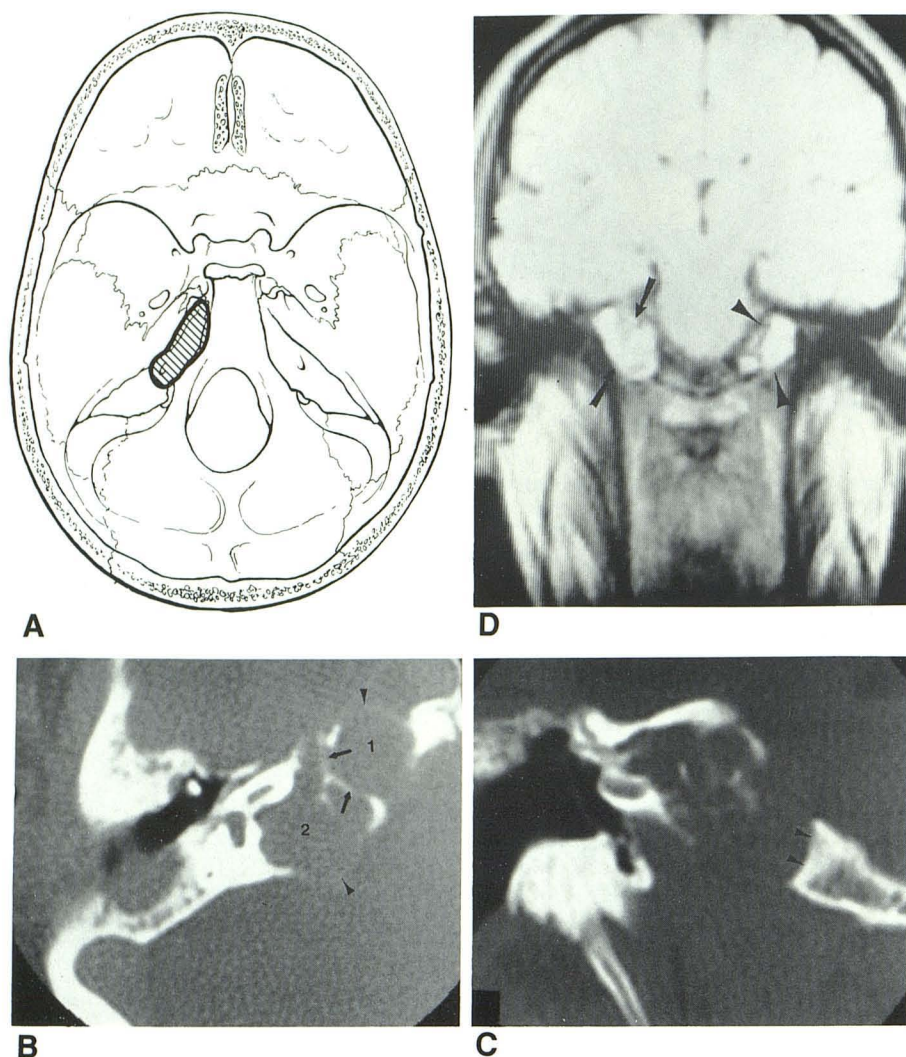


Fig. 4.—A, Giant cholesterol cyst on right (shaded area). B, Axial high-resolution CT scan. Two loculations of cyst (1 and 2) separated by bony remnants (arrows). Incomplete bony rim and scalloped bone margins again seen. Enhancement of wall demonstrates cyst bulging into middle and posterior cranial fossa (arrowheads). Chronic inflammatory and postoperative changes in mastoid area. C, Coronal high-resolution CT scan. Erosion by multiloculated cyst is most marked inferiorly. Bone remnants between loculations. Subtle occipital bone erosion present (arrowheads). D, Coronal MR image, 1 sec TR, 28 msec TE. High-signal lesion of right petrous apex (arrows). Similar abnormality on left also is presumed to be giant cholesterol cyst (arrowheads).

pathologic characteristics, *giant cholesterol cyst*, was suggested by Graham et al. [13].

The etiology of the giant cholesterol cyst is unknown, but air-cell obstruction either on a congenital or acquired basis appears a likely possibility [14]. Thus, this condition may be possible only in those petrous apices that are aerated [15]. In support of this theory, in the three patients with a normal opposite petrous apex, aeration was present. The fourth patient had bilateral petrous apex involvement. Residual air cells were found in two of the diseased petrous apices. Air-cell obstruction is also a likely etiology for mucocèles and cholesterol granulomas. These two lesions and giant cholesterol cysts may actually be very similar, representing different tissue responses to the same initial problem.

Giant cholesterol cysts initially destroy and expand the bone of the petrous apex. As they enlarge, they erode the bone of the posterior surface of the petrous bone and the adjacent occipital and sphenoid bones. Although abundant, the cholesterol crystals in the cyst fluid did not lower the CT attenuation below that of brain [16, 17]. The enhancement at the periphery

of the giant cholesterol cyst is in the cyst wall rather than in dura, since there is enhancement at the inferior extent of the cyst away from any dural surface. MR displays the high intensity of the cyst, without signal from the surrounding bone, and absence of a bone signal aids in the evaluation of such soft-tissue abnormalities of the temporal bone. Bone marrow, if present in the petrous apex, will yield a high signal with TRs and TEs the same as or similar to those used here and should not be confused with a lesion.

The differential diagnosis of a lytic lesion of the petrous apex is extensive. Somewhat arbitrarily, these lesions can be divided into primary lesions arising in the petrous apex and secondary lesions spreading to the apex [14]. Primary lesions comprise epidermoids (primary cholesteatoma), neuroma, bone or cartilage tumors (e.g., chondroma, osteoblastoma, etc.), petrous carotid aneurysm, rhabdomyosarcoma, histiocytosis X, and mucocèle. Secondary lesions comprise metastases, leukemia, lymphoma, chordoma, apical petrositis, glomus tumors, rhabdomyosarcoma, squamous cell carcinoma, meningioma, and neuroma. Most of the secondary lesions

and many of the primary lesions do not expand bone [18]. A reasonable differential diagnosis of an expanding lesion of the petrous apex should include giant cholesterol cyst, epidermoid, mucocele, petrous carotid aneurysm, neuroma, histiocytosis X, and primary bone or cartilage tumors [18–23]. Absence of bone or calcified cartilage matrix on high-resolution CT or tomography [20] and negative angiography will eliminate bone or cartilage tumors and a petrous carotid aneurysm, respectively [21]. Neuromas arising in the petrous apex may expand bone to the degree seen with the giant cholesterol cyst. On CT, however, neuromas usually enhance homogeneously or with small areas of central low attenuation [22]. Rimlike enhancement would be quite unusual with a neuroma. Histiocytosis X usually occurs in children and may involve other bones; a solitary lesion, however, could be radiographically identical to a giant cholesterol cyst [23]. The bony changes seen with mucocele may also resemble a giant cholesterol cyst. True mucocoeles with respiratory epithelium and mucus, however, are not only extremely rare but have not been reported to enhance on CT [6, 24]. Marked radiographic similarities exist between an epidermoid and the giant cholesterol cyst, and in this limited experience, they appear to be indistinguishable preoperatively [25–28].

Although a confident preoperative diagnosis of a giant cholesterol cyst may be impossible, knowledge of and anticipation of this lesion may result in simple drainage rather than a more radical procedure. Determination of the extent of the giant cholesterol cyst by high-resolution CT or tomography is also valuable in surgical planning.

The giant cholesterol cyst is a newly identified pathologic entity and, in our experience, the most common operable lesion of the petrous apex. Our initial limited experience indicates that it is not readily distinguishable from some other similar petrous apex lesions on preoperative imaging. However, awareness of and preparation for the possibility of a cystic lesion is important preoperatively and can influence the extent and approach to surgery.

ACKNOWLEDGMENTS

We thank Sandra Ressler for manuscript preparation and Spencer Phippen for medical illustrations.

REFERENCES

- Schaffer KA, Volz DJ, Haughton VM. Manipulation of CT data for temporal bone imaging. *Radiology* **1980**;137:825–829
- Waltner JG, Karatay S. Cysts of the mastoid bone. *Arch Otolaryngol* **1947**;46:398–404
- Nomura Y, Takemoto K, Komatsuzaki A. The mastoid cyst. Report of a case. *Laryngoscope* **1971**;81:438–446
- Gacek RR. Diagnosis and management of primary tumors of the petrous apex. *Ann Otol Rhinol Laryngol [Suppl]* **1975**;84[18]:1–20
- Montgomery WW. Cystic lesions of the petrous apex: trans-sphenoid approach. *Ann Otol* **1977**;86:429–435
- DeLozier HL, Parkins CW, Gacek RR. Clinical reports. Mucocele of the petrous apex. *J Laryngol Otol* **1979**;93:177–180
- House JL, Brackmann DE. Cholesterol granuloma of the cerebellopontine angle. *Arch Otolaryngol* **1982**;108:504–506
- Lo WEM, Solti-Bohman LG, Brackman DE, Gruskin P. CT diagnosis of cholesterol granuloma of the petrous apex. Presented at the annual conference on Radiology in Otolaryngology and Ophthalmology, San Antonio, May **1984**
- Gruber, cited by Johnson WR. The problem of the blue ear drum: idiopathic hemotympanum. *Laryngoscope* **1953**;63:1096–1117
- Shambaugh GE. The blue drum membrane. *Arch Otolaryngol* **1939**;10:238–240
- Sheehy JL, Linthicum FH, Greenfield EC. Chronic serous mastoiditis, idiopathic hemotympanum and cholesterol granuloma of the mastoid. *Laryngoscope* **1969**;79:1189–1217
- Nager GT, Vanderveen TS. Cholesterol granuloma involving the temporal bone. *Ann Otol* **1976**;85:204–209
- Graham MD, Kemink JL, Latack JT. Giant cholesterol cyst of the petrous apex. *Am J Otol* (in press)
- Flood LM, Kemink JL. Surgery of lesions of the petrous apex. *Otolaryngol Clin North Am* (in press)
- Schuknecht HF. *Pathology of the ear*. Cambridge, MA: Harvard University, **1974**:79
- Davis KR, Roberson GH, Taveras JM, New PFJ, Trevor R. Diagnosis of epidermoid tumor by computed tomography. *Radiology* **1976**;119:347–353
- Mikhael MA, Maltar AG. Intracranial pearly tumors: the roles of computed tomography, angiography, and pneumoencephalography. *J Comput Assist Tomogr* **1978**;2:421–429
- Lloyd GAS, Phelps PD, DuBoulay GH. High resolution computerized tomography of the petrous bone. *Br J Radiol* **1980**;53:631–641
- Lloyd GAS, Phelps PD. The investigation of petro-mastoid tumors by high resolution CT. *Br J Radiol* **1982**;55:483–491
- Gabrielsen TO, Kingman NF Jr. Osteocartilaginous tumors of the base of the skull. *AJR* **1964**;91:1016–1023
- Fisch V, Oldring D, Senning A. A surgical therapy of internal carotid artery lesions of the skull base and temporal bone. *Otolaryngol Head Neck Surg* **1980**;88:548–554
- Bergeron RT. The temporal bone. In: Bergeron RT, Osborn AG, Som PM, eds. *Head and neck imaging: excluding the brain*. St. Louis: Mosby, **1983**:728–841
- McCaffrey TV, McDonald TJ. Histiocytosis of the ear and temporal bone: review of 22 cases. *Laryngoscope* **1979**;89:1735–1742
- Osborn AG, Parkins JL. Mucocele of the petrous temporal bone. *AJR* **1979**;132:680–681
- Gacek RR. Evaluation and management of primary petrous apex cholesteatoma. *Otolaryngol Head Neck Surg* **1980**;88:519–523
- Olivecrona H. Cholesteatomas of the cerebello-pontine angle. *Acta Psychiatry Neurol* **1944**;24:639–643
- Paparella MM, Rybak L. Congenital cholesteatoma. *Otolaryngol Clin North Am* **1978**;11:113–120
- Cawthorne T, Griffith A. Primary cholesteatoma of the temporal bone. *Arch Otolaryngol* **1961**;73:252–261